Supplementary Material: Proto-cooperation: Group hunting sailfish improve hunting success by alternating attacks on grouping prey

Proceedings of the Royal Society B: Biological Sciences, DOI: 10.1098/rspb.2016.1671

James E. Herbert-Read[1,2,‡,*], **Pawel Romanczuk**[3,4,5,‡], **Stefan Krause**[6], **Daniel Strömbom**[1,7], **Pierre Couillaud**[8], **Paolo Domenici**[9], **Ralf H.J. M. Kurvers**[3,10], **Stefano Marras**[9], **John F. Steffensen**[11], **Alexander D.M. Wilson**[12,13], **Jens Krause**[3,4]

[1] Department of Mathematics, Uppsala University, 75106, Uppsala, Sweden, [2] Department of Zoology, Stockholm University, 10691, Stockholm, Sweden, [3] Leibniz-Institute of Freshwater Ecology and Inland Fisheries, Müggelseedamm 310, Berlin, Germany [4] Faculty of Life Sciences, Humboldt-Universität zu Berlin, 10115 Berlin, Germany, [5] Department of Ecology and Evolutionary Biology, Princeton University, Princeton, 08544 New Jersey, USA, [6] Department of Electrical Engineering and Computer Science, Lübeck University of Applied Sciences, 23562 Lübeck, Germany, [7] Department of Biology, Lafayette College, Easton, 18042, Pennsylvania, USA, [8] Département de la Licence Sciences et Technologies, Université Pierre et Marie Curie, 75005 Paris, France, [9] IAMC-CNR, Istituto per l'Ambiente Marino Costiero, Consiglio Nazionale delle Ricerche, Località Sa Mardini, 09170 Torregrande, Oristano, Italy, [10] Center for Adaptive Rationality, Max Planck Institute for Human Development, 14195, Berlin, Germany, [11] Marine Biological Section, University of Copenhagen, Helsingor, 3000, Denmark, [12] School of Life and Environmental Sciences, University of Sydney, Sydney, NSW, Australia 2006 [13] School of Life and Environmental Sciences, Deakin University, Waurn Ponds, Victoria, 3216, Australia,‡ These authors contributed equally to this study, ∗ E-mail: Corresponding author james.herbert.read@gmail.com

1 Empirical Observations

1.1 School size analysis

From the videos, we selected single frames of the sardine schools (n = 123 frames; 8 different schools; see Table S1 for number of images per school) to be analysed and exported them using VirtualDub (v 1.9.11). We imported the images into ImageJ (v 1.36b) and measured the lengths of five haphazardly selected fish in each image (in pixels) using ImageJ's internal measure function. We marked a polygon around the edge of the school's members and calculated the internal area of this polygon, again using the measure function. Dividing the area of this polygon (in pixels) by the average length of the five selected fish gave us a proxy for the relative size of each school (Fig. S1a). Sardine length is generally uniform across these schools [1].

1.2 Approach frequency

We recorded the time between consecutive approaches by different sailfish towards the sardine schools (n = 7 schools) (Fig. S1b). The time of approach was determined as the time when a sailfish was within one sailfish body length of the sardine school with its dorsal fin raised. This behaviour is typically observed before an imminent attack [1, 2]. If a sailfish was already approaching the sardine school at the very start of the video, we recorded the time of approach as zero. We also recorded the time at which this sailfish departed the school, which was defined as when the sailfish swam away from the school. The time between the approach and the departure was measured as the 'attack length'. We also determined the time between one sailfish departing and another sailfish approaching. On 19% of occasions, one sailfish approached the school before another sailfish had departed it. In these cases, one or both sailfish always abandoned their attack.

1.3 Injuries on individual fish

We investigated the extent to which individual sardines were injured. We sampled images from the videos where unobstructed individual injured fish could be seen. In each image, we selected 1- 2 individuals that were

visibly the most injured (n = 45). We only selected a fish if another fish obstructed less than $\sim$ 10% of its body surface. Like in the school injury analysis, but now based only on single individuals, we drew a polygon around the outline of the focal fish, calculated the area of the polygon and cleared all pixels from outside this polygon (making their intensity = 255). We then adjusted the brightness and contrast of each image before binary thresholding, and then imported these binary images into MATLAB. We then summed the number of pixels indicating injures (values equal to zero) and divided this total by the area of the polygon measured in ImageJ to determine the proportion of the body of a sardine that was injured.

1.4 Group size effects

Whilst we concentrated on how the sailfish progressively injured prey over time, and how capture rates were correlated with the level of injury in the prey school, there was also a weaker correlation between capture rates and school size (Spearman Correlation; ρ = -0.54, P = 0.24, n = 7). If indeed capture rates do increase as school size decreases (and we could not detect this effect due to limited sample size), then our model could be more broadly applied to other systems. The confusion effect decreases as group size decreases, sometimes making it easier to catch prey in smaller group sizes [3,4]. If individual hunters progressively decrease the size of the prey group over time, then this could allow hunters in the future to increase capture rates in subsequent attacks. Hence this model may not only apply when prey are injured or fatigued, but also when prey group size decreases over time.

1.5 Injury in the school

There was a negative trend between injury level and school size (Spearman Correlation; ρ = -0.69, P = 0.07, n = 8). Whilst again, the non-significant trend could be due to limited sample size, it may also be due to the dynamics of the hunt. Sailfish break off smaller schools from larger schools numbering into the hundreds of thousands of fish. If a small school was isolated relatively recently, it could in theory have a very low injury level compared to a larger group that had been under attack for a long time. Presumably our observed schools had variable initial sizes and attack durations that could introduce confounding variation into the levels of injury. We also note that our measure of the proportion of the school that was injured combines both the severity of injuries on individual fish, and the spread of injuries across different fish. Both the severity of injuries and spread of injuries across individuals are likely to be important in this system. We sometimes observed very injured sardines breaking off from the school, and these individuals were quickly consumed by the sailfish. Hence the level of injuries on singular fish are likely to be important for improving capture success rates as well as the general injury level of the school.

1.6 Why capture rates are likely to be important for group hunting sailfish

We identified that increased capture rates per unit time was a key benefit for individual hunters in groups. But why might these rates be important to increase, and why might hunting time be restricted? On two occasions we observed spotted dolphins, (*Stenella attenuata*), arriving at the sardine school that were under attack by sailfish. On arrival at the sardine school, the dolphins used their tails to stun and disperse the whole school. Sailfish that have potentially invested hours into injuring and exhausting their prey can thus lose their fish to the kleptoparasitic dolphins in a few seconds. The number of daylight hours is also likely to put an upper limit on available hunting time. Studies on tagged sailfish show that their time spent near the surface increases during the day (compared to the night) [5], which suggests that hunting primarily takes place at the surface during daytime periods. Hunting time is also likely to be constrained because once the targeted school has been consumed, the sailfish have to find another larger school, separate off a smaller school, and begin hunting again. Reducing the time between these events is presumably important in a time limited system. Further, because individual prey items are not shared, prey caught per unit time may be a particularly important measure of success during these hunts.

2 Modelling Group Hunting

2.1 Mathematical model - capture probability p_c

We assume that the capture probability p_c is a monotonically increasing function of the global injury level I, and is bounded by p_{min}, p_{max}: $0 \leq p_{min} \leq p_c(I) \leq p_{max} \leq 1$. There are infinitely many functions that fulfil these requirements, and based on our empirical observations, we have no *a priori* arguments to choose a particular one. However, the qualitative results will be independent on the particular choice of $p_c(I)$. Here we choose

$$p_c(I) = p_{min} + (p_{max} - p_{min})(1 - e^{-a_I I}) \tag{S1}$$

which increases linearly with I for small injury levels and approaches p_{max} asymptotically for $I \to \infty$ (see Fig. 2a, main text). This function naturally fulfils the monotonic increase in injury level with a necessary saturation level. We have also checked whether a nonlinear dependence of n_a on I affects our qualitative findings (see below, Sec 2.2). It is impossible to obtain a reliable value for the initial probability to catch a prey during a full attack sequence (approach to departure), but it appears to be very small. For simplicity we set $p_{min} = 0$. Therefore, if not otherwise stated, we use $p_{min} = 0$ and $p_{max} = 1$ as default parameters. We have checked that this simplification does not affect the qualitative results. Note that we cannot measure the global injury level I directly, and the fraction of prey school covered by injuries is only a visual proxy for I. Therefore it is advantageous to express p_c as a function of total number of attacks on the prey n_a.

The increment in the injury level ΔI per attack may in principle be an arbitrary function of the global injury itself: $\Delta I = g(I)$. This in general implies a nonlinear dependence of I on the number of attacks n_a: $I(n_a) = f(n_a)$. However, if we assume that the increment in the level of injury per attack is constant $\Delta I = const.$, then I is simply proportional to n_a ($I \propto n_a$). In this case we can set, without loss of generality, $\Delta I = 1$, rescale a_I to a new constant a, and replace I by n_a. The probability can then be directly expressed as a function of the number of attacks n_a as:

$$p_c(n_a) = p_{min} + (p_{max} - p_{\mathsf{min}})(1 - e^{-an_a}) \ . \tag{S2}$$

We have explored how the rate of increase of the capture probability, a, and p_{min} affects whether group hunting is beneficial for individuals in groups (Fig. S6). The main observation is a decrease of the maximal beneficial hunter group size with increasing p_{min}. The choice of a will strongly affect the overall time of the hunt before all prey individuals are captured and the average capture efficiency during the hunt (no. prey captured / no. attacks). Large values of a yield high average capture efficiencies already after a $1h$ of hunting ($p_c > 0.3$) and as a consequence very short hunts ($< 1h$) for reasonable prey school sizes. On the other hand extremely low values lead to very low initial capture efficiencies ($p_c \ll 0.1$) and eventually result in very long hunting times $> 4h$ (see Fig. S4). In combination with other parameters used, a choice of $a = 5 \cdot 10^{-4}$ yields total hunting times which appear consistent with our observations: $T \sim 2h$ for predator groups > 5.

2.2 Nonlinear dependence of injuries on number of attacks

In the main text, we assumed that the injury increment per attack is independent of the number of previous attacks, which implies a linear relationship between the number of attacks n_a and the prey injury level I. Here, we demonstrate that the qualitative results of our model remain unchanged for a nonlinear dependence of the injury level on n_a. We assume $I(n_a) = (\beta n_a)^\gamma$ with $\gamma > 1$. A direct consequence of such a nonlinear dependence is a sigmoid shape of $p_{catch}(n_a)$, where the function changes from convex to concave (change in sign of the second derivative) at a finite number of attacks. The factor β controls the location of the midpoint of the sigmoid ($p_{catch} = 0.5$), wheras the exponent γ determines the steepness of the sigmoid. In order to be able to compare results obtained for the linear and nonlinear model variants, we choose the additional nonlinear

parameters so that the cumulative capture probability $\sum_{j=0}^{n_a} p_{catch}(j)$ for $n_a = 2000$ attacks is approximately the same for both the nonlinear and linear model variant (see Fig. S7a).

In general, the nonlinear injury dependence results in a lower capture probability at low number of attacks in comparison to the linear case. This situation reverses for large n_a as p_{catch} increases strongly in the vicinity of the sigmoid midpoint before asymptotically approaching $p_{catch} = 1$ (Fig. S7a). As a consequence we expect in general lower capture rates at short times for all group sizes, as well as larger potential benefits from free riding at short hunting times. This is confirmed by the corresponding simulation results: First, we observe a very low capture success for small hunting group sizes and short hunting times (low accumulated number of attacks) as shown in Fig. S7b. In particular, this has a strong effect on the relative capture rate, normalised by the rate of solitary hunters. We observe a strong increase in the effective capture rates at short hunting times for group hunting, with respect to the number of prey a solitary hunter would have caught under the same conditions (Fig. S7c). Second, in the nonlinear case (see main text and Supplementary section 2.4 & 2.5), we observe an increased fitness benefit for free riders. This becomes particularly prominent at short hunting times (Figs. S8a,b) and yields a larger region in the energetic parameter space where free riding appears beneficial (Fig. S8c). However, our model predicts that also in the nonlinear case, free riding is unlikely to give fitness benefits for reasonable energetic parameters (in particular $c_0 \ll 0.5h^{-1}$).

2.3 Stochastic model with random attack and preparation times

In the main text we assume fixed, constant attack and preparation times. This yields perfect turn-taking of individuals with the order of attacking individuals set by the initial condition, which are randomised for each hunt. However, a perfect turn-taking behaviour may be questioned from a biological point of view. Furthermore, in general, deterministic temporal sequences may lead to pathological behaviour of mathematical models for certain parameter combinations ("resonances"). In order to confirm that our results are robust and independent on the turn-taking behaviour, we extended the simple model discussed in the main text, to random attack and preparation durations: Instead of fixed duration, we model the attack and preparation times as random variables t_a and t_r drawn from an exponential distribution with averages τ_a and τ_r, respectively. The initial order of attacking hunters is again random as in the main text, but now the order of the hunters within a single run does not persist but changes randomly due to the stochasticity of the attack and preparation durations. Figure S9 shows the comparison between the simulation results for the (scaled) number of prey captured for this modified model with our theoretical predictions (compare to main text, Fig. 2b and Fig. S5). All simulation results were obtained by averaging over 100 independent simulations. In particular for longer hunts (T large), only the average waiting times are relevant and the results of the fully stochastic model strongly match our theoretical predictions. For short times T, the additional stochasticity of the hunting process leads to smoothening of the maximum number of prey captured, but the position of the maximum and the maximal group size beneficial for hunting remain essentially unchanged.

2.4 Energy Balance Equation

As the detailed metabolic costs of swimming and attacking in sailfish are not documented, we considered a simple, yet generic model, where different energetic costs and benefits are summarised in a few key parameters. We assume that each hunter has a base rate of energy expenditure C_0, which includes all metabolic costs of swimming required to stay with the prey school, but excludes any additional energetic investment required to perform an actual attack sequence. For simplicity, we assume that attacks and captures are instantaneous events, which happen at discrete points in time t_a and t_c. This is a reasonable approximation as in general the average attack time τ_a will be much shorter than the total hunt time T_h. Prey capture is only possible during an attack, thus capture points t_c are always a subset of the attack points t_a. The additional costs of attack are included into the model as a constant energy decrement due to an increased energy consumption rate during an attack $\Delta E_a = C_a \tau_a$. The energy benefit from each captured prey is given by a constant increment ΔE_c. Thus the total energy E_i for an individual hunter i during a hunt evolves according to the following

balance equation:

$$\frac{dE_i(t)}{dt} = -C_0 - \Delta E_a \delta(t - t_a) + \Delta E_c \delta(t - t_c) \tag{S3}$$

$$= -C_0 - C_a \tau_a \delta(t - t_a) + \Delta E_c \delta(t - t_c) \tag{S4}$$

with $\delta(t - t')$ being the Dirac delta function. Without loss of generality, we rescale all terms by the energy increment due to prey capture ΔE_c, thus we measure the energy in units of the average energy content of a single prey item. The rescaled equation reads:

$$\frac{de_i(t)}{dt} = -c_0 - c_a \tau_a \delta(t - t_a) + \delta(t - t_c) \tag{S5}$$

with $e_i = E_i/\Delta E_c$, $c_x = C_x/\Delta E_c$.

By integrating over the entire time of the hunt T_h, we obtain the overall energy payoff per individual as:

$$\Delta e_{total,i} = -c_0 T_h - c_a \tau_a n_{a,i} + n_{c,i} \tag{S6}$$

with $n_{a,i} = \int_{t_0}^{t_0+T_h} \delta(t - t_a) dt$ and $n_{c,i} = \int_{t_0}^{t_0+T_h} \delta(t - t_c) dt$ being the number of attacks and the number of prey captured by the focal individual.

Finally we rewrite the energy payoffs by pulling out the base rate c_0 to obtain:

$$\Delta e_{total,i} = -c_0(T_h + \delta_c \tau_a n_{a,i}) + n_{c,i} \tag{S7}$$

Here the dimensionless number $\delta_c = c_a/c_0$ represents the effective increase of the energy consumption during an attack relative to the base consumption rate. A value of $\delta_c = 1$, would correspond to doubling of the energy consumption rate during an attack sequence. We discuss only biologically relevant parameter values c_0 and δ_c, where the average energy pay-offs are positive $\langle \Delta e_{total} \rangle > 0$. All other model parameters are the same as in the main text.

Because the routine metabolic rate of adult sailfish in unknown, we estimated a conservative value of c_0 based on the routine metabolic rate (RMR) of Blue-fin tuna (*Thunnus orientalis*). The RMR of a 8.1 kg tuna is $\sim$ 280 mg O_2 kg^{-1} h^{-1} at 25 ^{o}C [6]. The length:weight relationship of adult sailfish is given by: Log W $= -5.443L^{3.007}$ where W is the mass and L is the length of a sailfish [7]. A sailfish 240 cm in length, therefore, has a mass of 51.8 kg. We can scale the RMR of tuna according to the mass of the sailfish by the following scaling factor: $RMR_{sailfish} = RMR_{tuna}(8.1/51.8)^{(1-0.8)}$ [8, 9]. This gives a RMR for a sailfish as 193.2 mg O_2 kg^{-1} h^{-1}. This equates to a sailfish requiring 240 g O_2 per day. Given the oxycalorific coefficient is 13.59 [10], this equates to a sailfish requiring 3263 kJ of energy per day to maintain RMR. Domenici et al. (2014) found that the average length of sardines found in a sailfish's stomach was 19 cm [1]. This gives a mass of 57 g per sardine, based on their length:weight relationship [11]. The energy content of similar species (*Sardinops melanostictus* and *Clupea harengus pallasi*) is $\sim$ 6 - 9.6 kJ g^{-1} [12, 13]. An individual sardine, therefore, may provide 342 - 547 kJ of energy to a sailfish. Combining this information together, we estimate that a sailfish would require between 6 - 9.5 sardines per day to maintain RMR. This equates to $\sim$ 0.25 - 0.4 sardines per hour. Here we choose a value of $c_0 = 0.0001$, meaning that a sailfish would need to eat 1 sardine every 10000 seconds (2.8 hours, or 0.35 sardines per hour) to balance energy intake and expenditure. We note that with decreasing values of c_0, the free riding strategy becomes increasingly unlikely.

Another key question is; what is the realistic range of values for δ_c? Our earlier observations indicate that the speed of approach towards the prey school during an attack sequence is similar to the continuous swimming of non-attacking individuals [1,2]. However, sailfish sometimes initiate rapid swimming bursts when the school attempts to escape into the depths or when chasing single prey that have left the school. Thus significant additional energetic costs of an attack sequence can only originate from these burst swims, the slashing motion of the bill, turning, and prey handling, which are likely to only take-up a small fraction of the entire attack sequence. Even in the case of extremely high costs of slashing/capture, the relative increase in costs of an attack are most likely of the order of the base rate energy consumption ($\delta_c \sim 1 - 10$). It seems unlikely, therefore, that a free riding strategy could yield benefits to individuals.

2.5 Free riding during interrupted hunts

We also take into account the possibility of the hunt being interrupted due to external influences, for example, the arrival of other predators (e.g. dolphins). This is modelled by a constant probability p_{int} of the hunt being terminated. For $p_{int} = 0$, no interruption takes place and the hunt continues until all prey are captured. For finite $p_{int} > 0$ the hunt is interrupted randomly, and times available for hunting are exponentially distributed with the average time $T_h = 1/p_{int}$.

The qualitative findings do not depend on this model extension, and a significant energetic advantage of free riding can be observed only for very large δ_c values (Fig. S10). Interestingly, in these extreme cases with the finite probability of interruption of the hunt, the free rider advantage becomes more pronounced. This can be understood from the high energetic costs and negligible payoffs for producers in cases where the hunt was interrupted at an early stage.

References

1. Domenici P, et al. (2014) How sailfish use their bills to capture schooling prey. *Proc. Roy. Soc. B* 281:20140444.
2. Marras S, et al. (2015) Not so fast: Swimming behavior of sailfish during predator–prey interactions using high-speed video and accelerometry. *Integr. Comp. Biol.* 55:719–727.
3. Landeau L, Terborgh J (1986) Oddity and the confusion effect in predation. *Anim. Behav.* 34:1372–1380.
4. Ioannou C, Tosh C, Neville L, Krause J (2008) The confusion effect - from neural networks to reduced predation risk. *Behav. Ecol.* 19:126–130.
5. Hoolihan JP (2005) Horizontal and vertical movements of sailfish (*Istiophorus platypterus*) in the Arabian Gulf, determined by ultrasonic and pop-up satellite tagging. *Mar. Biol.* 146:1015–1029.
6. Blank JM, et al. (2007) Temperature effects on metabolic rate of juvenile pacific bluefin tuna *Thunnus orientalis*. *J. Exp. Biol.* 210:4254–4261.
7. Velayudham R, Veeramuthu S, Kesavan K (2012) Length-weight relationship and morphometrics of the sailfish, *Istiophorus platypterus* (Shaw & Nodder) from Parangipettai, Southeast coast of India. *Asian Pac. J. of Trop. Biomed.* 2:373–376.
8. Schurmann H, Steffensen J (1997) Effects of temperature, hypoxia and activity on the metabolism of juvenile atlantic cod. *J. Fish Biol.* 50:1166–1180.
9. Edwards R, Finlayson D, Steele J (1972) An experimental study of the oxygen consumption, growth, and metabolism of the cod (*Gadus morhua* L.). *J. Exp. Mar. Biol. Ecol.* 8:299–309.
10. Brett J, Groves T (1979) Physiological energetics. *Fish Physio.* 8:279–352.
11. FishBase (Accessed Jan 2016) Length-weight parameters for *Sardinella aurita*. *http://www.fishbase.se/PopDyn/LWRelationshipList.php?ID=1043&GenusName=Sardinella&SpeciesName=aurita&fc=43*.
12. Benoit-Bird K (2004) Prey caloric value and predator energy needs: foraging predictions for wild spinner dolphins. *Mar. Biol.* 145:435–444.
13. Anthony J, Roby D, Turco K (2000) Lipid content and energy density of forage fishes from the northern gulf of alaska. *J. Exp. Mar. Biol. Ecol.* 248:53–78.

3 Supplementary Figures

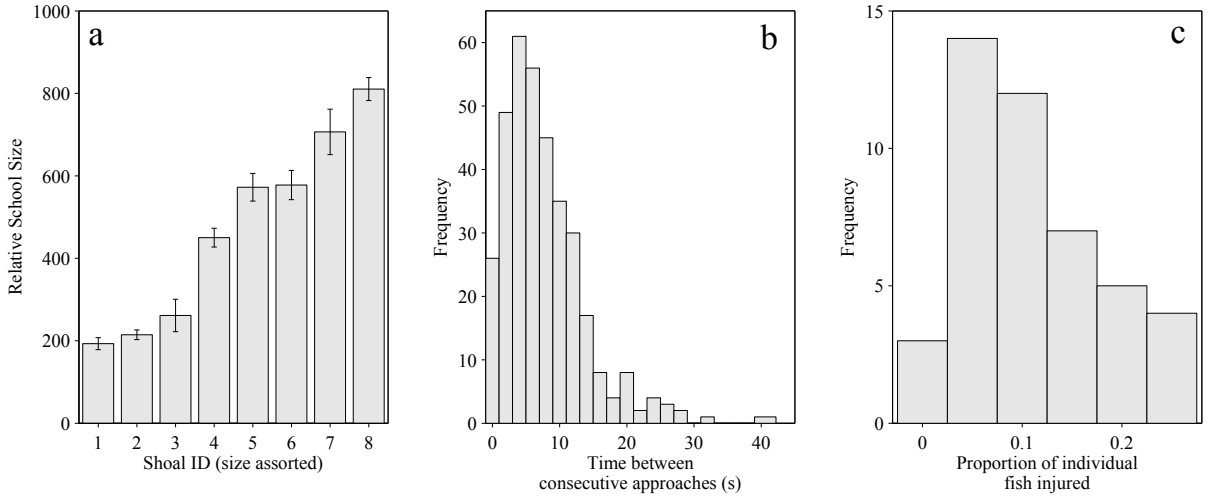

Figure S1. Empirical Data (a) Proxy of the sizes of the sardine schools we analysed. School 1 was composed of approximately 25 fish, whereas school 8 consisted of approximately 100-150 fish. Schools are ordered from smallest to largest (b) Distribution of the times between consecutive approaches by different sailfish towards the sardine schools. (c) The maximum proportion of injury on the bodies of individual sardines.

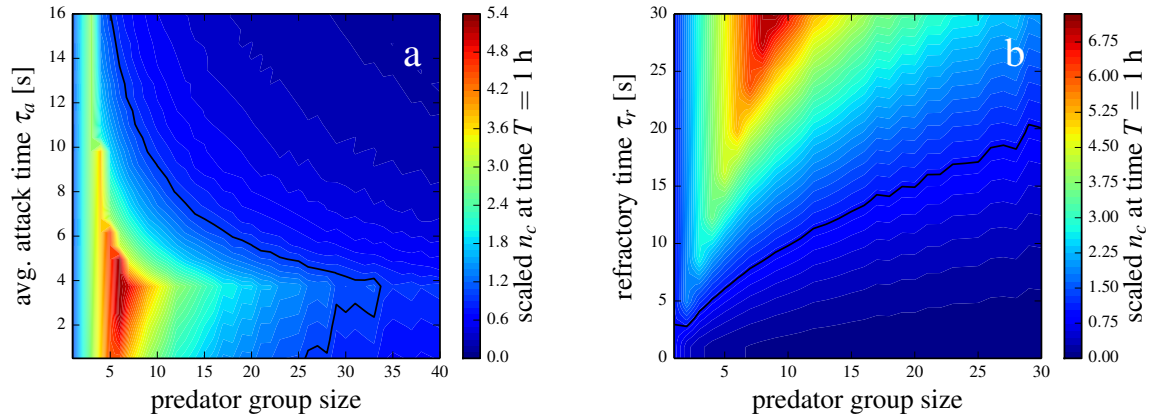

Figure S2. (a) Number of prey captured after time $T = 1h$ versus predator group size for varying the attack time τ_a and (b) varying the refractory time τ_r. n_c is normalised by the number of prey captured by a solitary predator. Solid lines show the contours corresponding to the value of $n_c = 1$ (same as solitary hunter) and represent therefore the border of the region where group hunting is beneficial. Default parameters as in the main text (if not varied): $p_{min} = 0$, $a = 5 \cdot 10^{-4}$, $\tau_a = 2.6$, $\tau_r = 20$, $S = 200$.

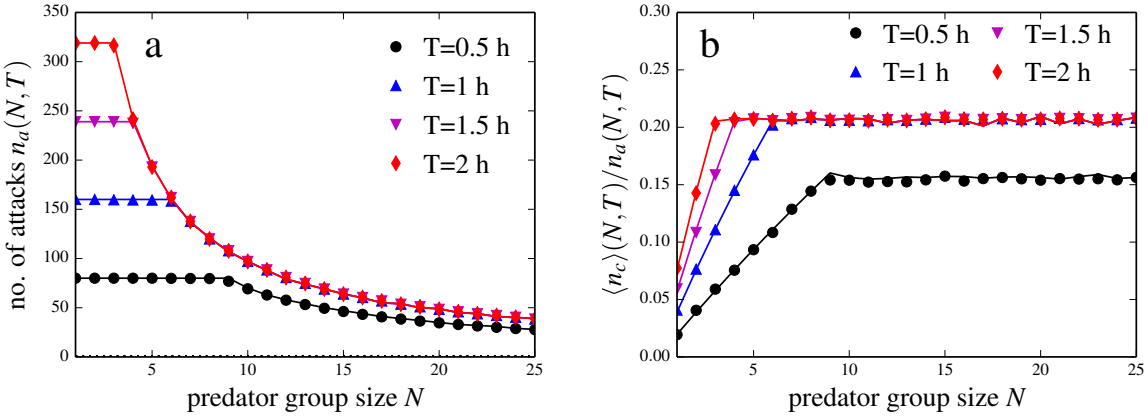

Figure S3. (a) Number of attacks per predator versus group size and (b) average number of prey captured per attack versus group size at different times T. Solid lines represent analytical predictions, whereas symbols represent results of model simulations. The number of attacks remains constant for $N < 1 + \tau_r/\tau_a$ - no temporal penalty of group hunting. For larger groups the number of attacks per individual decreases with group size as individuals have an increased idle time, where they have to wait until others perform their attacks. For all times, the average number of prey captured per attack increases initially with group size until $N = 1 + \tau_r/\tau_a$ and reaches a plateau for larger group sizes, as $\langle n_c \rangle$ (Fig. S5) scales in the same way as $n_a(N,T)$ (left) for large N. Parameters as in the main text: $p_{min} = 0$, $a = 5 \cdot 10^{-4}$, $\tau_a = 2.6s$, $\tau_r = 20s$, $S = 200$.

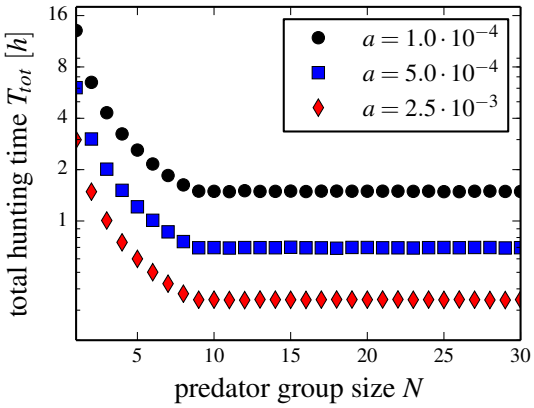

Figure S4. Total hunting time T_{tot} versus predator group size for different values of the p_c growth rate a (semi-logarithmic scale). The total hunting time decreases strongly for increasing predator group sizes ($N < 1 + \tau_a/\tau_r$), and then becomes independent of the group size N. It can vary from $6 - 8h$ for a solitary hunter to $1h$ for a groups larger than ten individuals. However, T_{tot} depends strongly on the choice of a. The blue line (squares) shows T_{tot} for parameters as used in the main text ($a = 5 \cdot 10^{-4}$). Other parameters as in the main text: $p_{min} = 0$, $\tau_a = 2.6s$, $\tau_r = 20s$, $S = 200$.

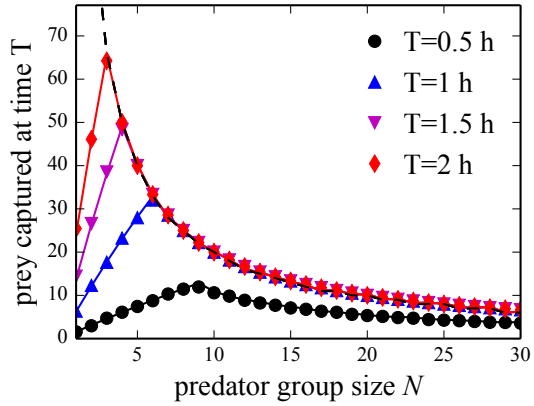

Figure S5. The number of fish captured by a single hunter as a function of group size N at different times, T, available for hunting, for parameters consistent with our experimental observations (for details on parameter choice see above). For short hunting times, capture success increases up to a maximum and then decreases monotonically with increasing N. For longer times and large N, the curves collapses on the limiting line set by the average number of prey per predator. Solid lines represent prediction of Eq. 1 taking into account the upper limit given S_0/N shown by the dashed line. Symbols represent the results of model simulation. Each point represents an average over 100 independent runs.

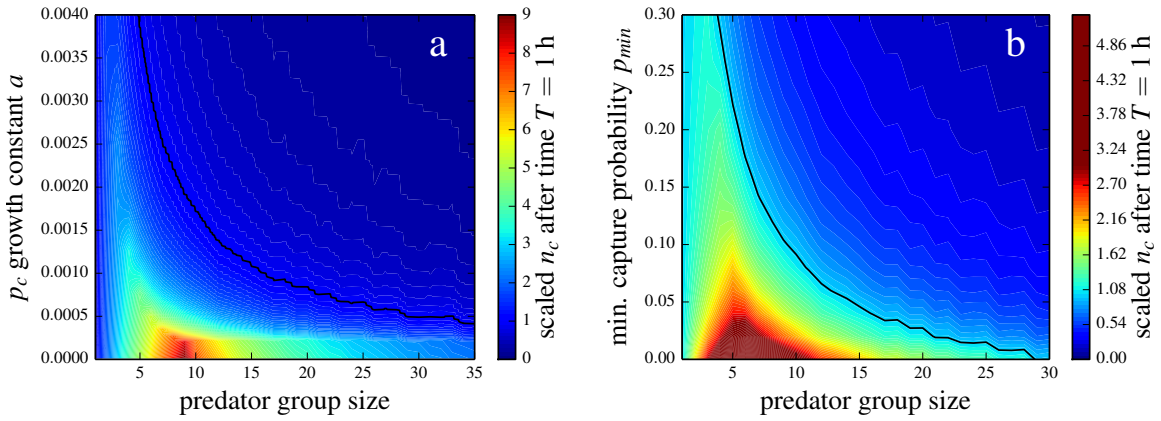

Figure S6. (a) Number of prey captured after a time $T = 1h$ versus predator group size for varying the growth rate of the capture probability a and (b) the min. capture probability p_{min}. n_c is normalised by the number of prey captured by a solitary predator. The second y-axis shows average capture probability per attack for a solitary hunter $\langle p_c \rangle_s$ calculated from the number of attacks of a solitary hunter required to catch 100 fish. Solid lines show the contours corresponding to the value of $n_c = 1$ (same as solitary hunter) and therefore represent the border of the region where group hunting is beneficial. Default parameters as in the main text (if not varied): $p_{min} = 0$, $a = 5 \cdot 10^{-4}$, $\tau_a = 2.6$, $\tau_r = 20$.

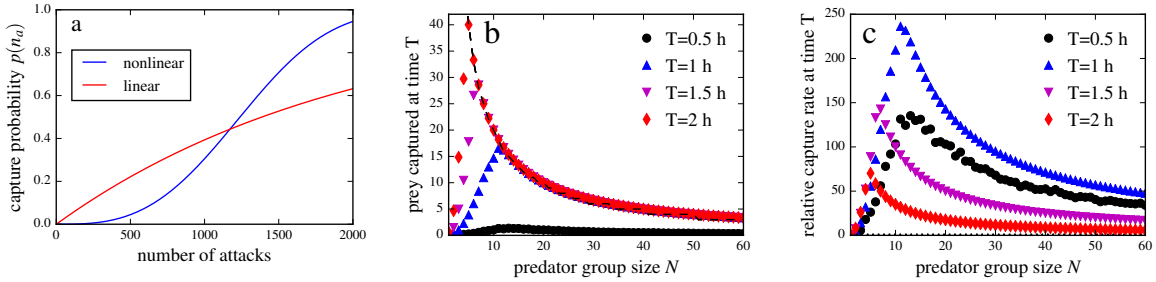

Figure S7. Nonlinear dependence of injury on number of attacks: (a) Comparison of the linear and nonlinear capture probability, where the factor β of the nonlinear model were chosen to match the cumulative p_{catch} for $n_a = 2000$ ($\gamma = 3$). (b) Absolute number of prey captured per hunter versus predator group size at different hunting times. (c) Relative capture rate versus groups size for different hunting times. All other simulation parameters as in the main text.

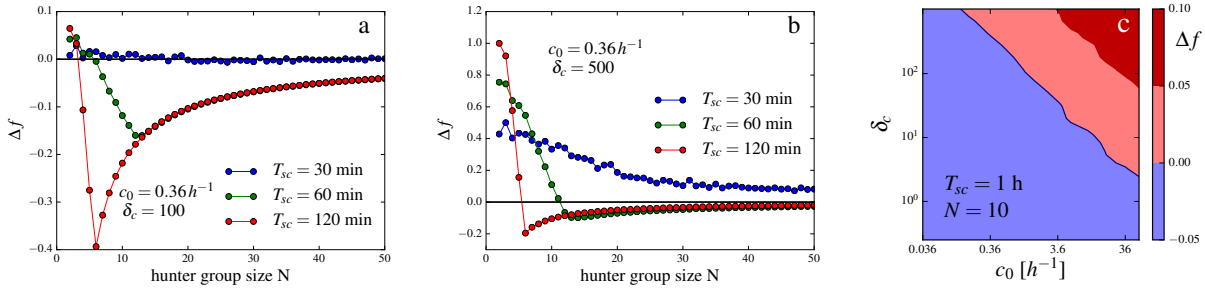

Figure S8. Nonlinear dependence of injury on number of attacks:: Relative fitness difference Δf with $c_0 = 0.36\text{h}^{-1}$ and different values of the relative energetic costs of attacks (a) $\delta_c = 100$, and (b) $\delta_c = 500$. (c) Δf versus c_0 and δ_c for fixed $T_{fr} = 0.5\text{h}$ and $N = 10$ (blue region indicates $\Delta f < 0$; i.e. where free riding is not beneficial). Parameters: $p_{int} = 0$ (no interrupt), $\gamma = 3$ and β chosen accordingly to match the cumulative p_{catch} for $n_a = 2000$ of the linear model; all other simulation parameters as in the main text.

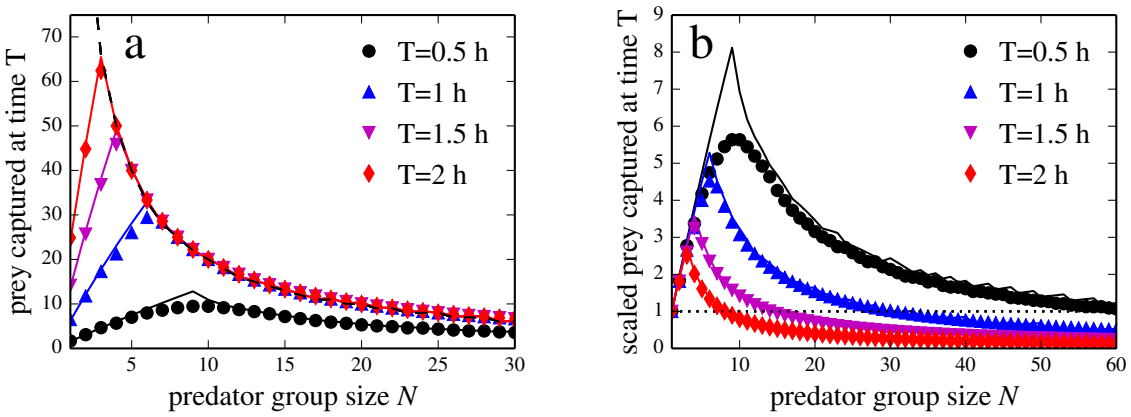

Figure S9. Group hunt model with stochastic attack and preparation times: (a) Number of prey captured per individual versus predator group size at different times available for hunting. Solid lines represent the prediction of Eq. 1 (main text) taking into account the upper limit given S_0/N shown by the dashed line. Symbols represent the results of model simulation. Each point represents an average over 100 independent runs. (b) Number of prey captured per individual as a function of N scaled by the number of prey captured for a solitary predator (horizontal dotted line). The largest group sizes, which offer an advantage to solitary hunting are typically observed for short times $T \leq 1h$ and decreases for large times (or small prey schools). For details on the modified model see section 1.3 above. Model parameters as in the main text: $\tau_a = 2.6s$, $\tau_r = 20s$, $a = 5 \cdot 10^{-4}$, $p_{min} = 0$, $p_{max} = 1$, $S_0 = 200$.

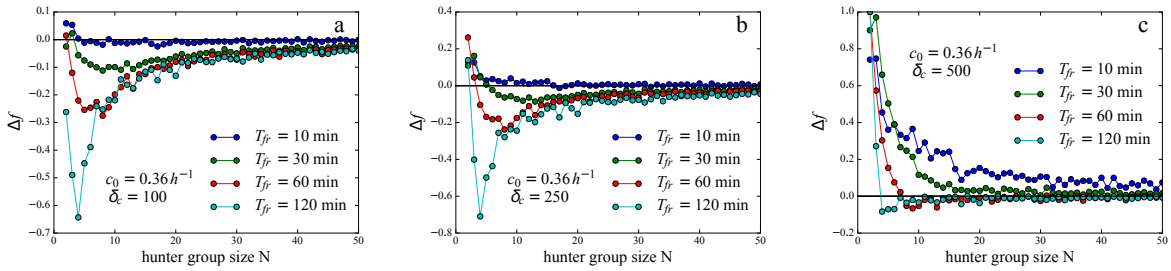

Figure S10. Relative fitness difference Δf for the extended model with the possibility of interruption of the hunt with $p_{int} = 0.0001$, with $c_0 = 0.36\text{h}^{-1}$ and different values of the relative energetic costs of attacks $\delta_c = 100$ (a), $\delta_c = 250$ (b) and $\delta_c = 500$ (c). All other simulation parameters as in the main text.

4 Supplementary Movies

Movie S1: One sailfish approaches and attacks a school of approximately 25 sardines. When the sailfish's bill makes contact with the sardines, the sardines' scales are removed. Note the injury marks on the sardines' bodies. The video is played at 1/8 of real time.

Movie S2: Sequence demonstrating that sailfish alternate attacks on their prey. Notice not all approaches results in attacks. Multiple prey are injured in the attack at 12 seconds, while only one sardine is caught. Not all attacks result in prey capture, for example, see attack at 27 seconds. Not all attacks result in prey being injured (attempted slash at 33 seconds). Also notice that sailfish tend to abandon attacks if they get out of position, or if another sailfish approaches the school at the same time. Video is played in real time.

Movie S3: An injured sardine break aways from the school and is quickly captured by a sailfish. The video is played at 1/8 of real time.

5 Supplementary Tables

School	#Images: School Size	#Images: Proportion of injuries
1	12	1
2	18	14
3	11	4
4	10	1
5	9	1
6	13	1
7	10	8
8	40	9

Table S1. Shoal identity and the number of images used to calculate school size or the number of images uses to calculate the proportion of injuries in the school.

Symbol	Description
Base Model	
N	number of predators
S_0	initial number of prey
τ_a	average time required to perform an attack sequence
τ_r	average time required to prepare for an attack sequence
p_{min}	capture probability at zero injury
p_{max}	maximal possible capture probability
a	growth rate of injury/capture probability with each attack
Model Extensions	
c_0	metabolic base rate measured in number or prey items per unit time
δ	increase of the energy consumption during an attack relative to the base rate
p_{int}	constant probability per unit time of the hunt being interrupted
γ	nonlinearity exponent for the dependence of injury levels on the number of attacks
β	nonlinearity factor

Table S2. Model parameters with description including parameters for the base model and the different extensions of the model discussed in the main text and supplementary information.